Published online 21 December 2016 *Nucleic Acids Research, 2017, Vol. 45, No. 7* **3707–3723**
doi: 10.1093/nar/gkw1285

Efficient DNA binding of NF-κB requires the chaperone-like function of NPM1

Jianhuang Lin[1,2], Mitsuyasu Kato[1,3], Kyosuke Nagata[2] and Mitsuru Okuwaki[1,2,*]

[1]PhD Program in Human Biology, School of Integrative and Global Majors, University of Tsukuba, 1-1-1, Tennodai, Tsukuba 305-8575 Japan , [2]Department of Infection Biology, Faculty of Medicine, University of Tsukuba, 1-1-1, Tennodai, Tsukuba 305-8575 Japan and [3]Department of Experimental Pathology, Faculty of Medicine, University of Tsukuba, 1-1-1, Tennodai, Tsukuba 305-8575 Japan

Received September 14, 2016; Revised November 21, 2016; Editorial Decision December 09, 2016; Accepted December 13, 2016

ABSTRACT

NPM1/nucleophosmin is frequently overexpressed in various tumors, although the oncogenic role of NPM1 remains unclear. Here we revealed the link between NPM1 and nuclear factor-κB (NF-κB), a master regulator of inflammation. We found that NPM1 knockdown decreased NF-κB-mediated transcription of selected target genes by decreasing the recruitment of NF-κB p65 to the gene promoters. NPM1 is directly associated with the DNA binding domain of p65 to enhance its DNA binding activity without being a part of the DNA–NF-κB complex. This result suggests that NF-κB requires the chaperone-like function of NPM1 for DNA binding. Furthermore, we demonstrated that NPM1 was required for efficient inflammatory gene expression induced by tumor necrosis factor alpha (TNF-α) and lipopolysaccharide in fibroblasts and macrophages. The NF-κB-mediated invasion of breast cancer cells was significantly decreased by NPM1 knockdown. Our study suggests a novel mechanistic insight into the NF-κB-mediated transcription and an oncogenic role of NPM1 in both tumor cells and the tumor microenvironment through the regulation of NF-κB.

INTRODUCTION

Tumorigenesis in human occurs through a multistep process in which normal human cells progress through a series of premalignant phenotypes until an invasive cancer emerges (1). During tumor development, cancer cells acquire distinctive and complementary hallmark capabilities that enable tumor growth and metastatic dissemination (2). In addition to cancer cells, tumors create the tumor microenvironment by recruiting normal cells that form the tumor-associated stroma to support tumor development, and progression as well as its drug resistance (3). Therefore, the tumor micro-environment has been considered to be a therapeutic target for anti-tumorigenesis treatment.

A transcription factor, nuclear factor-κB (NF-κB), plays a key role in tumor initiation, promotion, progression and metastasis (4–7). In addition to its oncogenic functions in cancer cells, NF-κB contributes to tumorigenesis through the activation of inflammatory cells in the tumor microenvironment because of its central role in the immune system. Therefore, NF-κB has been suggested to be a key link between inflammation and cancer. NF-κB was originally discovered as a site-specific DNA-binding protein complex that binds to the enhancer element of the immunoglobulin (Ig) kappa light-chain of activated B cells (8). The mammalian NF-κB family contains the following five proteins: (i) p65 (RelA); (ii) c-Rel; (iii) RelB; (iv) p50; and (v) p52, which function as homo- or hetero-dimers to control gene transcription (9). The most abundant form of the NF-κB complex contains the p65–p50 heterodimer that regulates the genes including those for cytokines, chemokines, adhesion molecules and enzymes that produce secondary inflammatory mediators.

Achieving precise and sufficient gene regulation by NF-κB requires specific post-translational modifications and interactions with cofactors (10). Indeed, it was predicted that the original size of the native NF-κB complex from nuclear extracts is much larger than that of the NF-κB p65–p50 heterodimer. Moreover, the native NF-κB complexes have a higher affinity for the Ig κB DNA motif than the reconstituted p65–p50 heterodimer does (11,12), which highlights the importance of cofactors for NF-κB DNA binding. It has been reported that ribosomal protein S3 (13), Sam68 (14), telomerase (15) and cyclin dependent kinase 6 (16) directly associate with the NF-κB complex and enhance its DNA binding activity. It was also observed that a nucleolar protein nucleophosmin/B23/NPM1 interacts with NF-κB and regulates the expression of the *SOD2* gene (17).

NPM1 is a highly abundant phosphoprotein that mainly resides in the nucleolus, but continuously moves between the nucleolus, the nucleoplasm, and the cytoplasm (18). We have identified NPM1 as a factor stimulating adenovirus

*To whom correspondence should be addressed. Tel: +81 298 537 950; Fax: +81 298 533 942; Email: mokuwaki@md.tsukuba.ac.jp

© The Author(s) 2016. Published by Oxford University Press on behalf of Nucleic Acids Research.
This is an Open Access article distributed under the terms of the Creative Commons Attribution License (http://creativecommons.org/licenses/by-nc/4.0/), which permits non-commercial re-use, distribution, and reproduction in any medium, provided the original work is properly cited. For commercial re-use, please contact journals.permissions@oup.com

chromatin remodeling and studied its functions in uninfected cells (19). It is a multifunctional protein involved in various cellular processes such as ribosome biogenesis (20,21), sperm chromatin remodeling (22), centrosome duplication (23) and DNA repair (24). Biochemically, NPM1 shows the histone chaperone activity (25), which is required for the regulation of chromatin structure. Histone chaperones bind directly to histones for their transfer to DNA to assemble chromatin without being incorporated into the chromatin. Much of the interest in NPM1 has been bolstered by the fact that it is directly implicated in tumorigenesis. On the one hand, the genetic alterations of the *NPM1* gene have been detected in various hematological malignancies, and strikingly, NPM1 is one of the most frequently mutated genes in acute myeloid leukemia (26). On the other hand, NPM1 is over-expressed in various solid tumors and has been proposed as a tumor marker (27). The expression levels of NPM1 have been reported to be regulated by the oncogene *MYC* (28) and to correlate with tumor recurrence and progression (29). However, the oncogenic functions of NPM1 remain still poorly understood in spite of the observations that NPM1 overexpression in tumor cells increases cell growth and proliferation, and inhibits cell differentiation and apoptosis (27).

Although the NF-κB pathway has been studied extensively and some of the cofactors of NF-κB have been identified, the molecular mechanisms by which the NF-κB activity is regulated by cofactors during cancer progression and inflammatory responses are not well understood. In the present study, we aimed to clarify the connection between two oncogenic proteins, NPM1 and NF-κB, to provide a new insight into the molecular basis of tumorigenesis. Our findings are important for two main reasons: (i) NF-κB, a master regulator of inflammation, requires the chaperone-like activity of an oncogenic protein NPM1 for its functions and; (ii) two oncogenic factors, NPM1 and NF-κB, are suggested to cooperatively regulate tumor progression through cancer cells and the tumor micro-environment.

MATERIALS AND METHODS

Plasmid constructs

NPM1 expression plasmids have been described previously (30). To construct pGEX2T-NPM1-ΔN, cDNAs for NPM1-ΔN was cut out from pET14b-NPM1-ΔN (30) by BamH I and cloned into the same site of pGEX2T vector. The p65/RelA, RelB, c-Rel, and p50 genes were cloned by PCR using primer sets 5′-ATGCGGATCCATGGACGAACTGTTCCCCCT-3′ and 5′- ATGCGGGATCCTTAGGAGCTGATCTGACTCA-3′, 5′-AAAGAATTCATGCTTCGGTCTGGGCCAGC-3′ and 5′-AAAGAATTCCTACGTGGCTTCAGGCCCCG-3′, 5′-AAAGGATTCATGGCCTCCGGTGCGTATAA-3′ and 5′-AAAGAATTCTTATACTTGAAAAAATTCAT -3′, and 5′-AAAGAATTCATGGCAGAAGATGATCCATA-3′ and 5′-AAACTCGAGTAGGTTCCATGCTTCATCCCAG-3′, respectively. The amplified p65, RelB, c-Rel, and p50 cDNA fragments were subcloned into the BamH I-digested, EcoR I-digested, BamH I and EcoR I-digested, and EcoR I and Xho I digested pcDNA3.1-Flag vector. The p65 and p50 cDNAs were also cloned into pcDNA3-HA vector. To construct vectors expressing p65 deletion mutants, deletion mutant cDNAs were cloned by PCR using primers 5′-ATGCGGATCCATGGACGAACTGTTCCCCCT-3′ and 5′-AAAGGATCCTTAAGAAAGGACAGGCGGCAGGC-3′ for p65-N1 (a.a.1–180), 5′-AAAGGATCCCATCCCATCTTTGACAATCG-3′ and 5′-AAAGGATCCTTAAGAAGCTGAGCTGCGGGAAG-3′ for p65-N2 (a.a.181–340), 5′-AAAGGATCCGTCCCCAAGCCAGCACCCCA-3′ and 5′-ATGCGGGATCCTTAGGAGCTGATCTGACTCA-3′ for p65-C (a.a. 341–551), p65 forward primer and p65-N2 reverse primer for p65-N (a.a.1–340), p65-N2 forward and p65 reverse primers for p65-N2C (a.a.181–551), the amplified cDNAs were subcloned into the BamH I sites of pcDNA3.1-Flag and pET14b vectors. All the plasmids were confirmed by DNA sequencing.

Animals, cell culture, transfection and reagents

C57BL/6J-$Apc^{Min/+}$ mice were purchased from the Jackson Laboratory. The *Min* pedigree was maintained by mating C57BL/6J wild-type females with C57BL/6J-$Apc^{Min/+}$males, genotype analysis was performed using a PCR assay as described (31). Colon adenomas were developed by administration of 2% dextran sulfate salt in drinking water for 7 days during 5th week of age. Mice were sacrificed at 8 weeks of age and subjected to histological analyses. BDF-1 mice were purchased from CLEA Japan, Inc. HeLa, HEK293T, BT-20, MDA-MB-157, MDA-MB-231, MDA-MB-436 cells, and $p53^{-/-}$ and $p53^{-/-}$NPM1$^{-/-}$ mouse embryonic fibroblast (MEF) cells were cultured in DMEM supplemented with 10% heat-inactivated fetal bovine serum (FBS) at 37°C with 5% CO_2. Primary macrophages were prepared from wild-type BDF-1 mice (10-week old) injected with 3.84% (w/v) thioglycollate 3 d after injection. PBS (5 ml) was injected into peritoneal cavity and recovered. Cells were centrifuged and seeded in RPMI1640 medium (GIBCO) supplemented with 10% FBS, and incubated at 37°C for 0.5 h. Non-adherent cells were removed by wash with PBS, and cells were maintained in the same medium.

Transfection and reagents

Transfection of plasmid DNA and siRNAs were performed by GeneJuice (Novagen) and Lipofectamine RNAiMAX (Life technologies), respectively, according to the manufacturer's instructions. Stealth RNAs for negative controls and human NPM1 were described previously (32). Mouse NPM1 (s124573) and human NF-κB p65 (HSS109159) were obtained from Life technologies. Antibodies used were NPM1 (Invitrogen), Flag tag (M2, Sigma Aldrich), p65 (ab7970, Abcam), I-κBα (sc-371, Santa Cruz) and β-actin (sc-47778, Santa Cruz). Recombinant human TNF-α (PEPROTECH) and Lipopolysaccharide (LPS) (Sigma) were commercially available.

Preparation of proteins

Purifications of GST-tagged proteins and his-tagged proteins were described previously (33). For purification of

Flag-tagged proteins, HEK 293T cells transfected with appropriate expression vectors were suspended in buffer A (0.1% Triton X-100, 20 mM Tris-HCl pH7.9, 10 mM KCl, 1.5 mM $MgCl_2$, 0.5 mM phenylmethylsulfonyl fluoride (PMSF)) containing 400 mM NaCl on ice for 10 min and rotate at 4°C for 30 min followed by centrifuge at 15k rpm, 4°C for 15 min. The supernatants were recovered and diluted with twice volumes of buffer A without NaCl. The cell extracts were incubated with anti-Flag M2 affinity gels (SIGMA–ALDRICH) for 2 h at 4°C and then washed by buffer B (0.1% Triton X-100, 50 mM Tris-HCl pH7.9, 0.5 mM PMSF) containing 300 mM NaCl. The proteins bound with the resin were eluted with buffer A containing 150 mM NaCl and Flag peptide (SIGMA–ALDRICH), dialyzed against buffer H (20 mM Hepes–NaOH pH 7.9, 50 mM NaCl, 0.5 mM ethylenediaminetetraacetic acid, 1 mM Dithiothreitol (DTT), 0.1 mM PMSF and 10% Glycerol).

Immunoprecipitation and GST-pull down assay

HeLa cells were treated with or without TNF-α and the cell lysates were prepared. The extracts were subjected to immunoprecipitation with control Ig or anti-p65 antibody, and immunoprecipitated proteins were separated by sodium dodecyl sulphate-polyacrylamide gel electrophoresis (SDS-PAGE) and detected by western blotting. For GST-pull down assays, GST, GST-NPM1 or GST-NPM1 deletion mutants was incubated with glutathione-sepharose beads in buffer A for 45 min and washed with buffer A twice. The beads were mixed with Flag-p65, RelB or c-Rel and incubated at 4°C for 2 h followed by extensive washing with the same buffer. Proteins were eluted from the beads by an SDS sample buffer, separated by SDS-PAGE, and visualized by CBB staining and western blotting.

Reporter assay

HeLa cells (3×10^4 per well) were seeded in 24-well plates and transfected with 80 ng of pNF-κB-TA-Luc (Firefly luciferase) and 20 ng of pTA-RL (*Renilla* luciferase) at 48 h after transfection with siRNA for NPM1 or negative control. Sixteen hours after transfection, cells were treated with 20 ng/ml TNF-α for different time courses as described in the legend. Luciferase assay was performed using *Renilla* Luciferase Assay System kit (Promega Corporation, USA) according to the manufacturer's instructions. The sane experiments were performed with $p53^{-/-}$ and $p53^{-/-}NPM1^{-/-}$ MEFs.

RT-qPCR and chromatin immunoprecipitation (ChIP) assays

Total RNA was extracted using RNeasy Kit (Qiagen) according to the manufacturer's instructions. cDNA was prepared from purified RNA (1 μg) by using ReverTraAce (Toyobo) with oligo dT primer. Real-time PCR was carried out in triplicate with primers (sequences are shown in Supplementary Table S1) by using SYBR Green Realtime PCR Master Mix-Plus (Toyobo) in the Thermal Cycler Dice Real-Time PCR system (TaKaRa). ChIP was performed with HeLa cells treated with or without TNF-α. Cells were fixed with 1.4% formaldehyde at room temperature for 10 min, the whole cell lysates were sonicated to generate DNA fragments 200–1000 base pairs in length. The sonicated lysates were used for ChIP with anti-p65, anti-NPM1 or IgG control antibodies. After washing, the complexes were eluted, protein–DNA crosslink was reversed, and DNA was purified and used for quantitative PCR. Primer sequences used for PCR were shown in Supplementary Table S2.

EMSA

Double-stranded oligonucleotide probes containing the κB sequences derived from *immunoglobulin* (*Ig*), *IL-8* and *NR4A2* genes (see Figure 6D) were used. The mutant *Ig* κB (5′-AGTTGAATCCACTTTCCCAGG-3′) were also used for electrophoretic mobility shift assay (EMSA). For *Ig* κB sequence, the oligonucleotide was [^{32}P]-labeled and used for EMSA assay as previously described (13). Briefly, p65 or p50 protein (20 ng/sample) was incubated with the purified GST, GST-NPM1 or His-NPM1 protein at 25°C for 30 min, followed by additional incubation with [^{32}P]-labeled Ig κB (WT) or Ig κB (Mut) oligonucleotide at 25°C for 30 min. Samples were resolved on a 6% native PAGE in 0.5xTBE buffer. For supershift analyses, recombinant proteins were preincubated with 0.2 μg of antibodies for 20 min on ice prior to the addition of labeled probes.

Immunofluorescence, proximity ligation assays, immunohistochemistry

The cells on cover slips were fixed with 3% paraformardehyde in PBS, permeabilized in PBS containing 0.5% Triton X-100 and incubated with anti-NPM1 and p65 antibodies diluted with PBS containing 0.5% non-fat dry milk. Localization of proteins was visualized with secondary antibodies conjugating with AlexaFluor dyes (Molecular Probes). During final wash with PBS containing 0.1% Triton X-100, DAPI DNA staining dye was added and incubated for 15 min at room temperature. *In situ* proximity ligation assay (PLA) kit (Sigma-ALDRICH) was used to detect protein–protein interaction in fixed cells according to the manufacturer's instructions. PLA signals were quantitatively analyzed by the image processing software Imaris (Carl Zeiss microimagining). Localization of proteins, DNA and PLA signals was observed under confocal microscope (LSM EXCITER; Carl Zeiss Microimaging, Inc.). For immunohistochemistry assay, $Apc^{min/+}$mice (12-weeks old) were given 2% (w/v) DSS in drinking water for 1 week, then changed to normal drinking water for 2 weeks. Colon tissues from the mice were cut and opened, fixed in phosphate-buffered 10% formalin and embedded in paraffin and cut into 5-μm sections. The sections were dewaxed, rehydrated and immersed in 3% hydrogen peroxide for 20 min to quench endogenous peroxidase activity. Antigen retrieval was performed at 95°C for 20 min in sodium citrate buffer (pH 6.0). The sections were incubated with blocking buffer (PBS supplemented with 2% goat serum and 1% bovine serum albumin) for 1 h, anti-NPM1 or p65 antibodies for 1 h, a biotinylated secondary antibody for 45 min and peroxidase-conjugated streptavidin solution for 45 min. Protein local-

ization was visualized with 3, 3-diaminobenzidine and sections were lightly counterstained using Gill's haematoxylin.

Microarray hybridization and data analysis

HeLa cells were incubated with NPM1 or control siRNA for 72 h and treated without or with 20 ng/ml TNF-α for 2 h. Total RNA was then isolated using RNeasy Kit (Qiagen) according to the manufacturer's instructions. The sense-strand cDNA was prepared using Ambion WT Expression Kit from 200 ng total RNA. The cDNA was then fragmented and labeled using the Affymetrix GeneChip WT Terminal Labeling Kit. The fragmented and labeled cDNA was injected to the Gene Arrays 1.0 ST and incubated at 45°C with 60 rpm for 17 h. The hybridized samples were washed and stained using Affymetrix fluidics station 450. GeneChips were scanned using Affymetrix GeneArray Scanner 3000 7G Plus. All kits were obtained from Affymetrix (Santa Clara, CA, USA) and experiments were performed according to the manuals. Raw data were analyzed using the rma() function in R-Bioconductor (34) package 'affy' (35,36) with default setting. Background correcting was processed by the RMA (robust multichip averaging) (37), the data were normalized by quantiles and the signal intensity of each probe set was obtained by the method medianpolish. The annotation of probe sets was performed by Bioconductor hugene10sttranscriptcluster.db. The microarray data are available at the NCBI Gene Expression Omnibus (GEO) under accession number GSE81785. Gene ontology analysis was performed using DAVID (The Database for Annotation, Visualization and Integrated Discovery) (http://david.abcc.ncifcrf.gov/) (38,39).

Matri-gel invasion assay

Invasion assays were performed using transwell chambers (24-well insert; pore size, 8 μm; Corning-Costar, Corning, NY, USA). Transwell membrane was coated with 30 μg of matrigel and incubated at 37°C for 3 h. MDA-MB-231 cells (5×10^4) in 200 μl of serum-free medium were seeded into the upper chamber of the transwell and medium supplemented with serum was used as a chemoattractant in the lower chamber. The cells on the upper chamber were treated with or without TNF-α, incubated for 16 h and cells that did not invade through the pores were removed with a cotton swab. Cells on the lower surface of the membrane were fixed with methanol and stained with 0.05% crystal violet. The stained cells were counted under a microscope (Leica Dmi8) in three random fields/well.

RESULTS

Interaction between NPM1 and NF-κB

A previous study showed that NPM1 interacts with the NF-κB subunits p65 and p50 (17). However, whether NPM1 also interacts with other NF-κB family proteins and the interaction is direct or not have never been examined. We first examined the interaction between NPM1 and the NF-κB family Rel proteins, p65 (RelA), RelB and c-Rel. Flag-tagged p65, RelB and c-Rel were purified (Figure 1A) and a glutathione S-transferase (GST) pull down assay was performed. All purified Flag-tagged p65, RelB and c-Rel were more efficiently precipitated with GST-NPM1 than GST, indicating that NPM1 directly interacts with the NF-κB proteins *in vitro*. Flag-p65 precipitated by GST-NPM1 was much more efficient than RelB and c-Rel (Figure 1B), suggesting that NPM1 preferentially associates with p65. We also found that NPM1 directly interacted with p65 and p50 (Supplementary Figure S1). We next confirmed the endogenous interaction between NPM1 and the NF-κB p65 subunit by co-immunoprecipitation with anti-p65 antibody in HeLa cells treated without or with TNF-α (Figure 1C). Endogenous NPM1 was weakly co-immunoprecipitated with p65 without TNF-α treatment, whereas the co-immunoprecipitated NPM1 was increased upon TNF-α treatment. Furthermore, *in situ* PLA using antibodies for both NPM1 and p65 revealed that NPM1 interacted with p65 mainly in the nucleus (Figure 1D, top panels). Treatment of cells with TNF-α, which activates the NF-κB pathway, dramatically enhanced the interaction (Figure 1D, bottom panel and Figure 1E). The PLA signals were mainly detected in the nucleoplasm, indicating that this is where the interaction between p65 and NPM1 occurred. These results indicated that NPM1 interacts with NF-κB in the cells and this interaction is enhanced by treatment of cells with TNF-α. Because NPM1 is mainly localized in the nucleolus, we tested whether NPM1 localization was changed upon treatment of cells with TNF-α. HeLa cells stably expressing enhanced green fluorescent protein (EGFP)-NPM1 were treated with TNF-α and the localizations of p65 and EGFP-NPM1 were examined (Figure 1F). p65 was translocated to the nuclei 15 min after TNF-α treatment. We found that although the interaction between p65 and NPM1 occurred in the nucleoplasm (Figure 1D and E), TNF-α treatment did not clearly change the localization of EGFP-NPM1.

NPM1 regulates NF-κB-dependent gene transcription

We next examined the effect of RNAi-mediated knockdown of NPM1 on the expression of NF-κB-dependent reporter gene expression in HeLa cells. NPM1 siRNA significantly decreased the total amount of NPM1 compared with the non-specific (NS) control siRNA (Figure 2A). The reporter activity was found to be decreased by NPM1 knockdown even in the absence of TNF-α. As expected, TNF-α treatment induced the NF-κB-driven luciferase activity in NS siRNA-treated cells, but this induction was significantly decreased in NPM1 siRNA-treated cells (Figure 2B).

We performed microarray analysis to comprehensively analyze the effect of NPM1 knockdown on the NF-κB-dependent gene expression induced by TNF-α treatment in HeLa cells. We found that without TNF-α treatment, 288 genes were upregulated (>1.5-fold) and 359 genes were downregulated (<0.667-fold) by NPM1 knockdown (Supplementary Figure S2B and Table S4), suggesting that NPM1 is involved in the regulation of a variety of genes. Upon stimulation with TNF-α, 77 genes were upregulated (>1.5-fold) and 13 genes were downregulated (<0.667-fold) (Supplementary Figure S2A and Table S3). In addition, in TNF-α treated cells, NPM1 knockdown decreased the

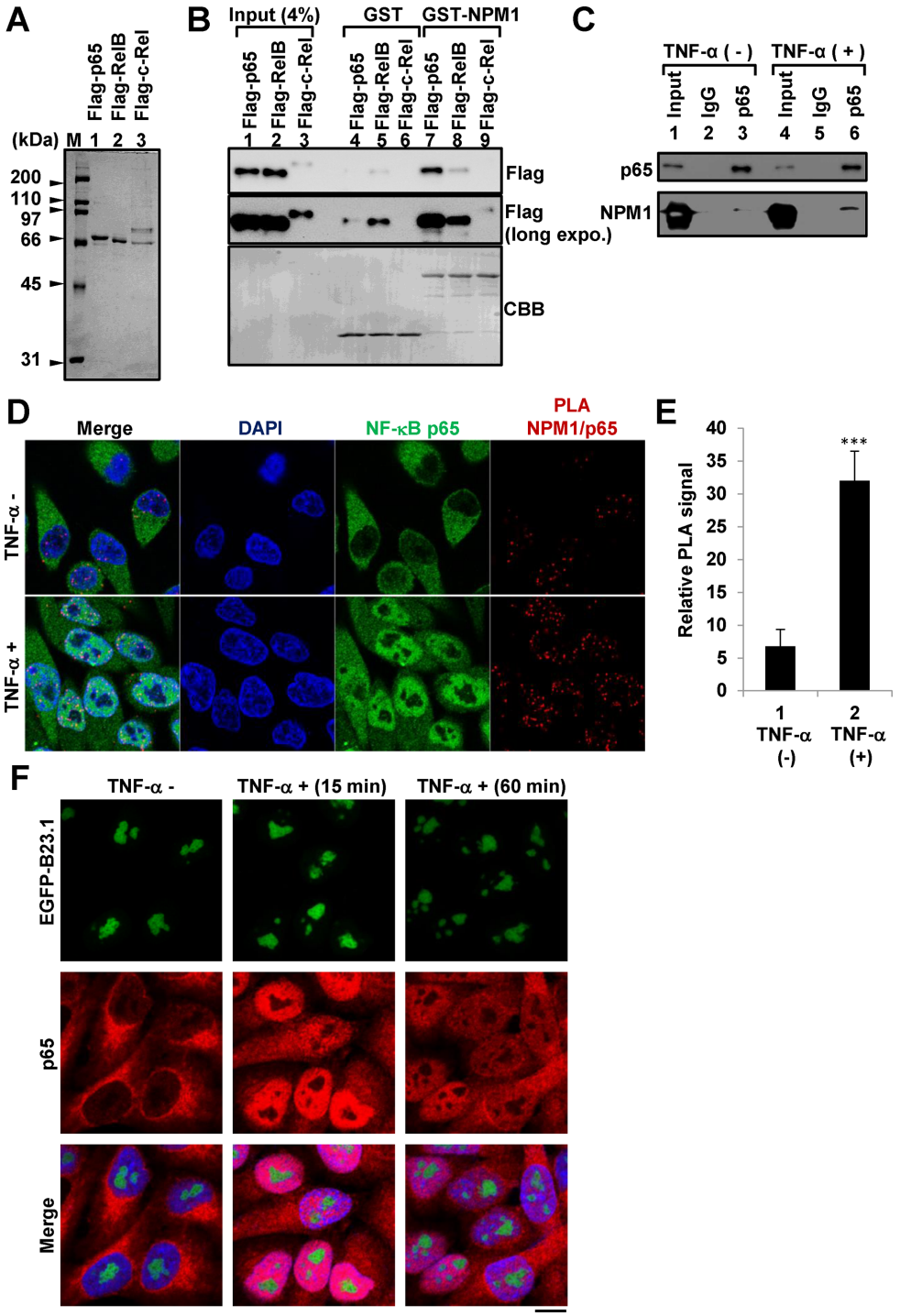

Figure 1. Interaction between NPM1 and NF-κB. (**A**) Purified NF-κB proteins. Flag tagged p65, RelB and c-Rel were expressed in 293T cells, purified with Flag-affinity gel, separated by 10% SDS-PAGE and visualized by CBB staining. (**B**) Direct interaction between NPM1 and the NF-κB proteins. GST pull-down assays using GST or GST-NPM1 (lanes 4–6 and 7–9) with purified Flag-p65 (RelA), -RelB or -c-Rel were performed. Flag-tagged NF-κB proteins were detected by western blotting and the GST proteins were visualized by CBB staining. (**C**) Immunoprecipitation assay. Cell extracts were prepared from HeLa cells treated without or with TNF-α for 30 min, and the interaction between NPM1 and p65 was analyzed by immunoprecipitation with control Ig and anti-p65 antibody. The input (lanes 1 and 4) and immunoprecipitated (lanes 2, 3, 5 and 6) proteins were separated by SDS-PAGE and analyzed by western blotting with anti-NPM1 and p65 antibodies. (**D** and **E**) *In vivo* interaction between NPM1 and p65. HeLa cells were treated with or without 20 ng/ml TNF-α for 1 h, *in situ* proximity ligation assays (PLAs) were performed using primary antibodies against NPM1 and p65. The PLA signals in panel C were quantitatively analyzed by the image processing software Imaris. The average spot number per cell was calculated from randomly selected cells ($n = 20$). Error bars represent ±SD, statistical significance was calculated using student's *t*-test and *** indicates $P < 0.001$. (**F**) Localization of NPM1 in TNF-α treated cells. HeLa cells stably expressing EGFP-NPM1 were treated without or with TNF-α (20 ng/ml) for 15 min and 60 min, followed by immunofluorescence analysis with anti-p65 antibody and the localization of the proteins was observed by a confocal microscope. Bar at the bottom indicates 10 μm.

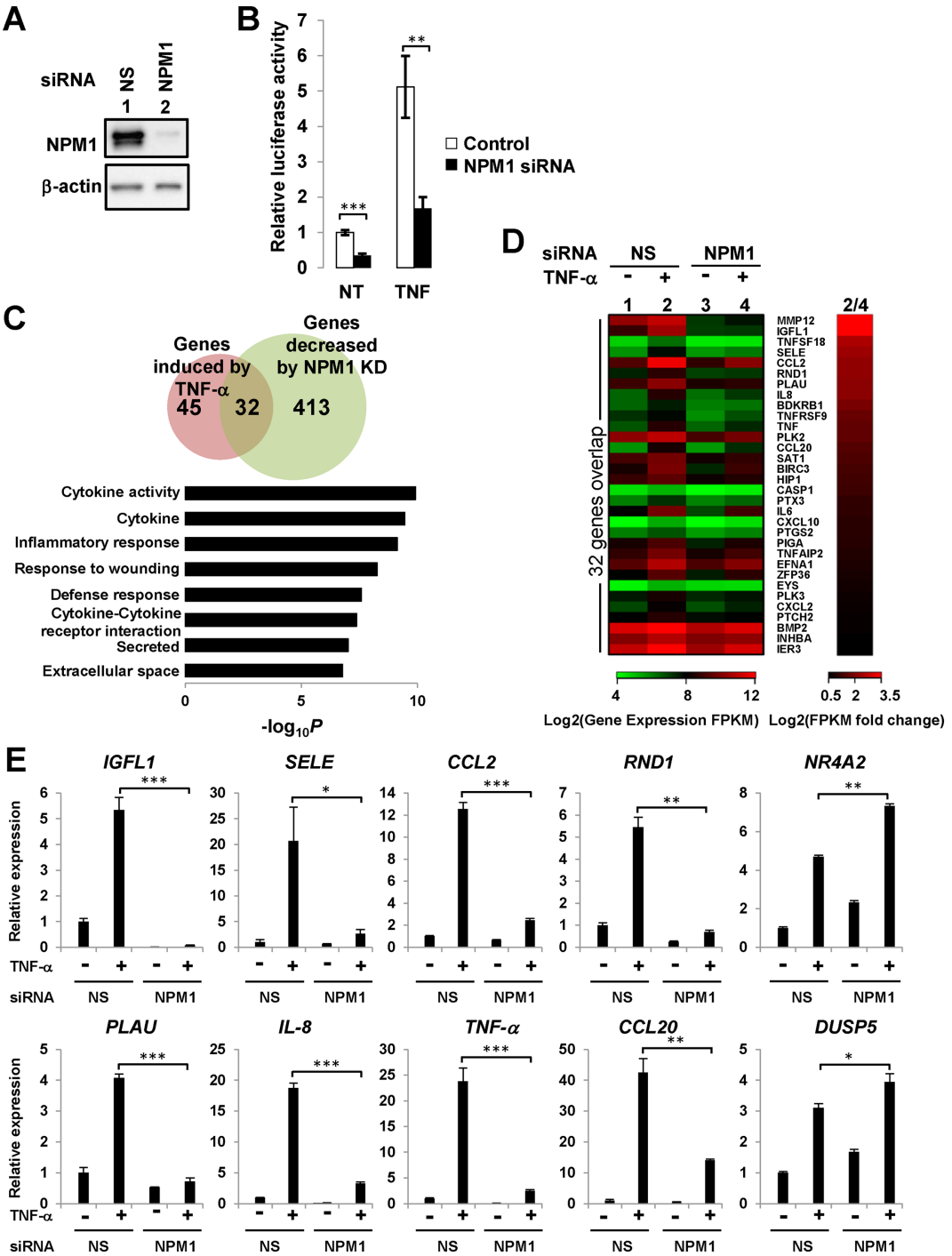

Figure 2. NPM1 regulates NF-κB-dependent gene transcription. (**A**) Knockdown of NPM1 in HeLa cells by siRNA treatment. Western blotting confirmed the knockdown of NPM1 in HeLa cells. β-actin is a loading control. (**B**) Reporter assay. HeLa cells treated with NS or NPM1 siRNAs were transfected with p-κB-uc and p-TA-RL plasmids. The cells were then stimulated without or with TNF-α for 3 h and subjected to luciferase assay. The relative luciferase activity (fold increase) is shown. Three independent experiments were performed and error bars indicate ±SD. (**C** and **D**) Microarray analyses. RNAs were extracted from HeLa cells treated with control siRNA (chip 1 and 2) or NPM1 siRNA (chip 3 and 4) followed by stimulation without (chip1 and 3) or with TNF-α (chip 2 and 4), and subjected to microarray analyses. The Venn diagram (upper panel) shows the coding genes induced by TNF-α treatment (chip 1 versus 2), the coding genes downregulated by NPM1 knockdown in cells treated with TNF-α (chip 2 versus 4) and their overlapped genes. The overlapped 32 genes were subjected to gene ontology analysis and the list of the enriched functions is shown. Heat maps (D) depict the expression of the 32 overlapped genes (left) and the fold changes (right) between control and NPM1 knockdown cells treated with TNF-α (chip 2 versus 4). The data are more precisely shown in Supplementary Figure S2D. (**E**) Confirmation of the microarray data by real-time RT-PCR analyses. RT-PCR for the genes involved in the list of (D) was performed using RNA extracted from cells treated with or without siRNAs and TNF-α as indicated at the bottom. RT-PCR was also examined for the two genes (*NR4A2* and *DUSP5*) that were upregulated by NPM1 knockdown, three independent experiments were performed and error bars indicate ±SD. The results were statistically analyzed by student *t*-test and ***, ** and * represent $P < 0.001$, 0.01 and 0.05, respectively.

expression of 445 genes (<0.667-fold) and increased the expression of 223 genes (>1.5-fold) (Supplementary Figure S2C and Table S5). Among the 77 genes upregulated by TNF-α treatment, 32 genes were downregulated (>1.5-fold) by NPM1 knockdown (Figure 2C, upper panel) and only two genes were upregulated (>1.5-fold) by NPM1 knockdown. When the cutoff fold-change (chip2 versus chip4) was set to 1.2, the number of the genes downregulated by NPM1 knockdown was increased to 55, while only seven genes were upregulated (>1.2-fold) by NPM1 knockdown (Supplementary Figure S2E and F). These results suggested that NPM1 is involved in the regulation of most, but not all, genes stimulated by TNF-α treatment. The heat map shows the expression of the 32 genes sorted by the fold change values (Figure 2D and Supplementary Figure S2D) between control and NPM1 knockdown in TNF-α-treated cells. Many of them are cytokines, such as *IL-8*, *TNF-α*, and *IL-6*. Indeed, gene ontology (GO) analysis of the 32 TNF-α-induced genes whose expressions were downregulated (>1.5-fold) by knockdown of NPM1 showed functional enrichment in inflammation and immunity such as cytokine activity, cytokine, inflammatory response, response to wounding and defense response (Figure 2C, lower panel). To confirm the microarray analyses, reverse transcriptase-mediated polymerase chain reaction (RT-PCR) was performed (Figure 2E). The expressions of eight genes (*IGFL1*, *SELE*, *CCL2*, *RND1*, *PLAU*, *IL-8*, *TNF-α*, and *CCL20*) were confirmed to be significantly reduced by NPM1 knockdown. In addition, we confirmed that the expression levels of *NR4A2* and *DUSP5* were slightly increased by NPM1 knockdown. It should be noted that the increase or decrease of those genes was observed even in the absence of TNF-α treatment. To further confirm the specific effect of NPM1 on the NF-κB pathway, we next examined the NF-κB-mediated gene expression in control and EGFP-NPM1 expressing HeLa cell lines (Supplementary Figure S3A). Over-expression of NPM1 significantly increased the expressions of NF-κB target genes *TNF-α* and *RND1* both in NS and NPM1 siRNA treated cells, whereas those of *NR4A2* and *DUSP5* genes were slightly decreased (Supplementary Figure S3B). These results support the idea that NPM1 is involved in the regulation of NF-κB-mediated transcription and the effect of NPM1 knockdown on NF-κB dependent transcription is not due to the off-target effect of siRNA.

To explore the mechanism by which NPM1 regulates the expression of the genes stimulated by TNF-α, we examined whether NPM1 knockdown affected the NF-κB signaling pathway such as I-κB protein degradation, NF-κB nuclear translocation and NF-κB recruitment to its target genes upon stimulation by TNF-α. The I-κB proteins bind NF-κB to retain it in the cytoplasm and are quickly degraded upon stimulation by TNF-α through the ubiquitin-proteasome system to allow the nuclear translocation of NF-κB. The *I-κB* genes are target genes of the NF-κB complex and the I-κB–NF-κB complex constitutes a feedback oscillatory circuit (40). Indeed, I-κBα was quickly degraded upon TNF-α treatment and the expression was recovered within 60 min, and the oscillatory expression was observed with peak expressions at 60 and 105 min (Figure 3A). We found that I-κBα protein degradation was similarly observed 15 min after TNF-α stimulation regardless of the level of NPM1 expression (lane 2). However, the pattern of oscillatory expression of I-κBα was changed by NPM1 knockdown, suggesting that NPM1 is involved in the I-κBα expression. Likewise, the nuclear translocation of NF-κB p65 upon TNF-α treatment was not affected by knockdown of NPM1 (Figure 3B). We then examined whether NPM1 affected the binding of NF-κB to target gene promoters by chromatin immunoprecipitation (ChIP). In unstimulated cells, a low but distinct amount of p65 was detected at the promoter regions of *TNF-α*, *PLAU*, *IL-8*, *NR4A2* and *DUSP5* genes. Upon stimulation with TNF-α, the binding of p65 to these genes was significantly increased. However, NPM1 knockdown decreased the p65 binding to the *TNF-α*, *PLAU* and *IL-8* gene promoters in both unstimulated and TNF-α-stimulated cells. In contrast, the recruitment of p65 to the promoter regions of *NR4A2* and *DUSP5* was not affected by knockdown of NPM1 (Figure 3C). These results indicate that NPM1 stimulates the binding of NF-κB to a subset of NF-κB target gene promoters. We noted that the expression of *NR4A2* and *DUSP5* was increased by NPM1 knockdown regardless of TNF-α treatment (Figure 2E and Supplementary Figure S3), whereas the promoter binding of p65 to these genes was not significantly affected. These results indicate that NPM1 suppresses these genes independent of the promoter binding of NF-κB.

NPM1 enhances the DNA binding activity of NF-κB

Considering the effect of NPM1 on the binding of NF-κB to target gene promoters *in vivo* and its direct interaction with NF-κB *in vitro*, we next examined whether NPM1 affected the binding of NF-κB to the κB site *in vitro* by the EMSA using purified recombinant NF-κB proteins and His-NPM1 (Figure 4A). When either Flag-p65 or Flag-p50 was expressed, a homo-dimer of Flag-tagged proteins and a minor population of a heterodimer of Flag-tagged proteins and endogenous p65 or p50 were purified (lanes 2 and 3). When Flag-p50 and HA-p65 were co-expressed and purified with anti-Flag affinity gel, the Flag-p50 homodimer and the heterodimer of Flag-p50 and HA-p65 were purified (lane 4). All purified p50 homodimer, p65 homodimer and p65–p50 heterodimers specifically bound to the κB oligonucleotide (Figure 4B, lanes 2 and 5), but not to the mutant κB oligonucleotide (lanes 3 and 6). The addition of anti-p65, anti-Flag tag or anti-HA tag antibody induced supershift, thereby ensuring the binding of specific NF-κB dimers to the κB oligonucleotide (lanes 4 and 7–9). NPM1 significantly increased the binding of all NF-κB dimers to the κB oligonucelotide in a dose dependent manner, whereas NPM1 itself did not bind to the κB oligonucleotide (Figure 4C).

To test whether NPM1 is included in the NF-κB/DNA complex, EMSA with or without anti-NPM1 was performed (Figure 4D). The Flag-p65 homodimer and Flag-p50–HA-p65 heterodimers were bound to the κB oligonucleotide, which was enhanced by NPM1 (lanes 2, 3, 6 and 7). The addition of Flag antibody, but not NPM1 antibody, induced a supershift of the complex containing DNA and the NF-κB proteins (lanes 4, 5, 8 and 9). Considered together, these results indicated that NPM1 binds directly

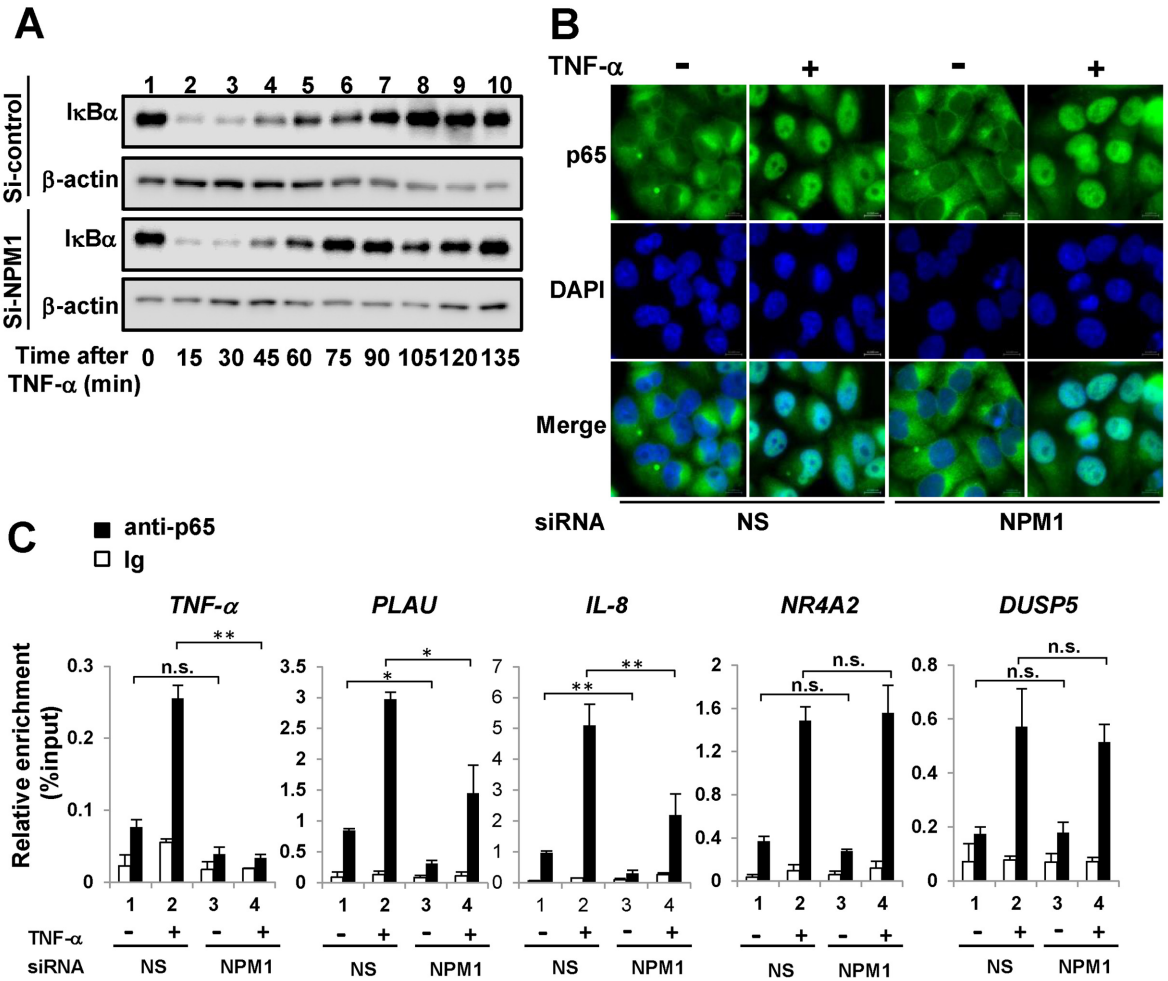

Figure 3. NPM1 regulates the target gene binding of NF-κB, but not its nuclear translocation. (**A**) Effect of NPM1 knockdown on the expression level of I-κBα. The amounts of I-κBα and β-actin in HeLa cells treated with control siRNA or NPM1 siRNA after TNF-α treatment were examined by western blotting. Time (min) after TNF-α treatment is shown at the bottom of the panel. (**B**) Localization of p65 after TNF-α treatment in HeLa cells treated with control or NPM1 siRNA. DNA was counter stained by DAPI. (**C**) Recruitment of p65 to its target genes. HeLa cells transfected with siRNAs as indicated were incubated without or with TNF-α for 1 h, followed by ChIP assay. The precipitated DNA amounts containing the promoter regions of the genes listed in Figure 2D (*TNF-α*, *PLAU* and *IL-8*) and those of stimulated genes (*NR4A2* and *DUSP5*) by NPM1 knockdown were quantitatively analyzed by q-PCR. Three independent experiments were performed and error bars indicates ±SD. The results were statistically analyzed by student *t*-test and ***, ** and * indicate $P < 0.001$, 0.01 and 0.05, respectively.

to and enhances the DNA binding activity of the NF-κB proteins without being incorporated into the NF-κB/DNA complex.

To further explore whether NPM1 is incorporated into the NF-κB/DNA complex *in vivo*, we next performed ChIP assays with antibodies against endogenous p65 and NPM1 (Figure 4E). The binding of p65 to the *PLAU* and *IL-8* gene promoters, but not to the *ribosome RNA* gene (rDNA), was increased upon TNF-α treatment in a time-dependent manner. NPM1 showed constant binding to rDNA as previously reported (20), but was not recruited to the *PLAU* and *IL-8* gene promoters during the entire time course after TNF-α treatment. These results support our conclusion that NPM1 is not included in the NF-κB/DNA complex. In addition, it is unlikely that NPM1 stimulates the p65 binding by regulating the histone density on the NF-κB target genes as a histone chaperone, because NPM1 itself does not stably associate with the NF-κB target genes.

NPM1 and κB DNA compete for binding to NF-κB

We next attempted to clarify the mechanism by which NPM1 enhances the DNA binding activity of NF-κB. To this end, we first determined the NF-κB binding domain of NPM1 by a GST-pull down assay with the NPM1 deletion mutant proteins (Figure 5A). A splicing variant of NPM1/B23.1 termed B23.2 that lacks the C-terminal RNA binding domain interacted with p65, indicating that the C-terminal RNA binding domain is dispensable for p65 binding (Figure 5B, lane 7). Further analyses suggested that the N-terminal oligomerization domain and acidic regions were also dispensable for p65 binding and the C-terminal region termed NPM1-CR was sufficient to interact with p65 *in vitro* (Figure 5B, lanes 2–6).

Next, the NPM1 binding domain of p65 was determined by immunoprecipitation assay. Flag-tagged p65 proteins were expressed in 293T cells and immunoprecipitated

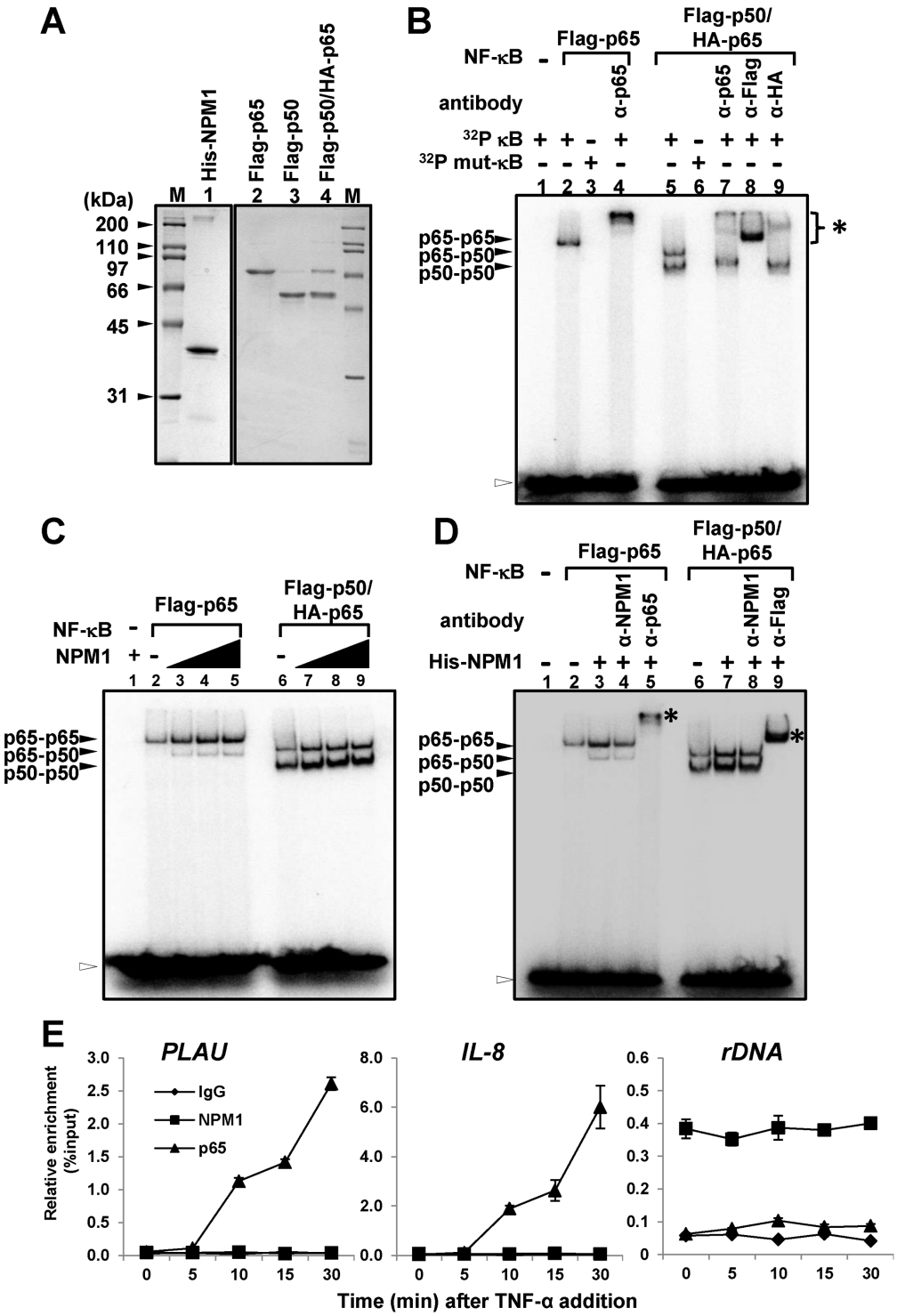

Figure 4. NPM1 enhances the DNA binding activity of NF-κB. (**A**) Purified proteins. His-tagged NPM1 and the NF-κB proteins purified with Flag-tag antibody were separated by SDS-PAGE and visualized by CBB staining. (**B**) EMSA with purified proteins. Purified recombinant NF-κB proteins (20 ng/sample) were analyzed by EMSA with a [^{32}P]-labeled, double-stranded wild-type (WT) or mutant (mut) κB oligonucleotides (300 fmole/sample). Antibodies against p65, Flag-tag or HA-tag were added in the mixture as shown in lanes 4 and 7–9. (**C**) Effect of NPM1 on the DNA binding activity of the NF-κB proteins. Flag-p65 and Flag-p50/HA-p65 (20 ng, lanes 2–5 and 6–9, respectively) were incubated with increasing amounts of His-NPM1 (0, 50, 100 and 200 ng), followed by EMSA with [^{32}P]-labeled probe (200 fmole/sample). The NPM1 alone (200 ng) was also incubated with the same probe (lane 1). (**D**) Supershift analysis with NPM1 antibody. Flag-p65 and Flag-p50/HA-p65 (20 ng, lanes 2–5 and 6–9, respectively) were incubated without or with His-NPM1 (200 ng) and indicated antibodies, followed by EMSA. The DNA bands bound by the p65–p65, p65–p50 and p50–p50 complexes, free probes and supershifted bands are indicated by filled arrowheads, blank arrowheads and asterisks, respectively (B–D). (**E**) Chromatin immunoprecipitation assay. HeLa cells were treated with TNF-α (20 ng/ml) for indicated time periods and then subjected to ChIP assays with control Ig, anti-p65 and anti-NPM1 antibodies. The *rRNA* gene coding region (*rDNA*) and the promoter regions of *PLAU* and *IL-8* genes were analyzed by qPCR.

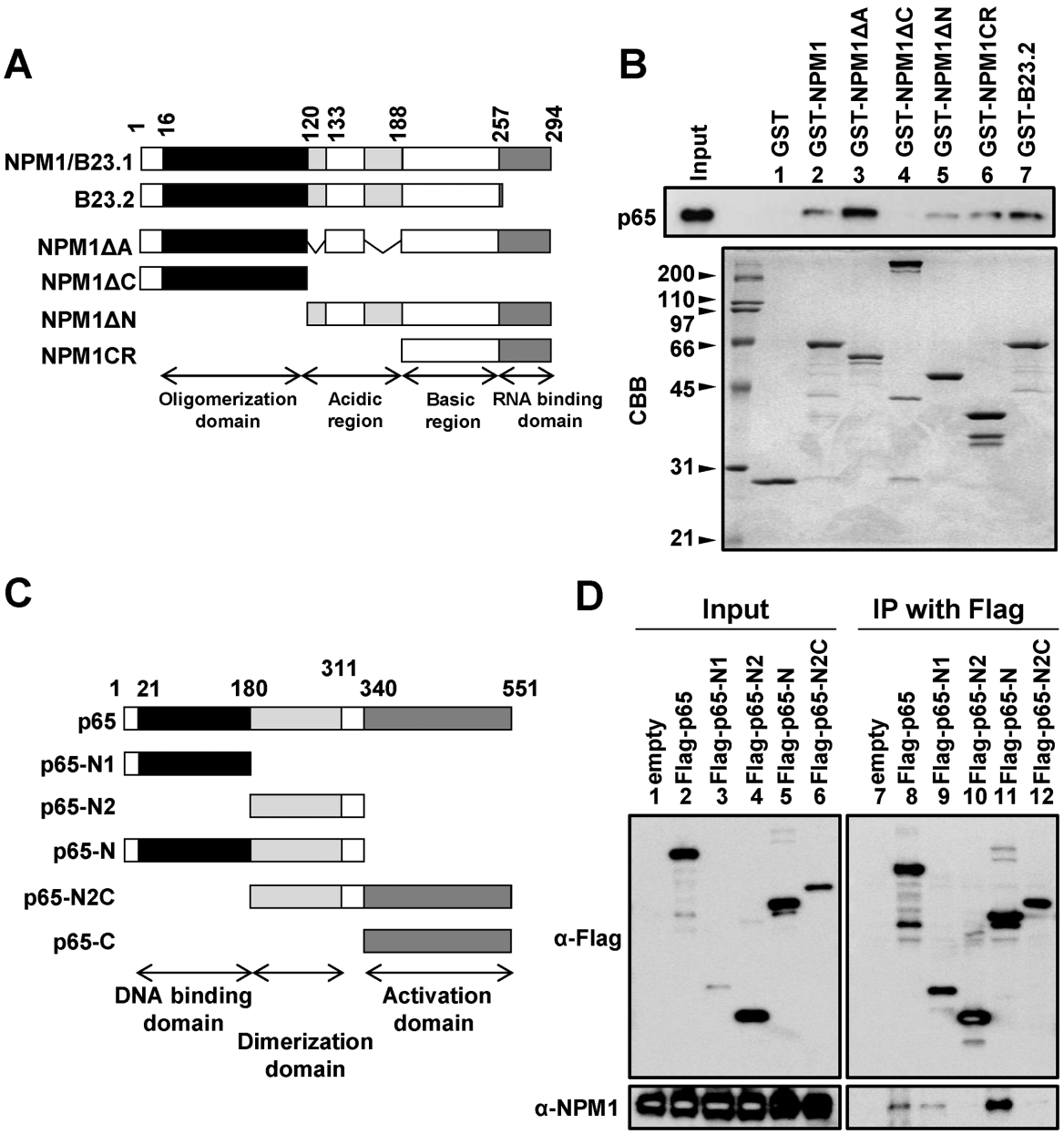

Figure 5. The domain mapping of NPM1 and p65 required for their interaction. (**A**) Diagram of the splicing variants and truncation mutants of NPM1. Black, light gray and dark gray boxes indicate oligomerization domain, acidic regions and the C-terminal globular domain, respectively. (**B**) GST-pull down assay. GST or GST fusion proteins were incubated with purified Flag-p65 (500 ng/sample) and the bound proteins were analyzed by SDS-PAGE, followed by CBB staining for GST proteins (bottom panels) or western blotting with anti-Flag antibody (top panels). (**C**) Diagram of the mutants of p65. The N-terminal DNA binding domain, dimerization domain and the activation domain are shown by black, light gray and dark gray boxes, respectively. (**D**) Immunoprecipitation analysis of the Flag-tagged p65 mutant proteins. Flag-tagged wild-ype and truncated p65 proteins were transiently expressed in 293T cells and immunoprecipitated with anti-Flag antibody. Input and immunoprecipitated proteins were analyzed by western blotting with anti-Flag and -NPM1 antibodies.

with anti-Flag antibody followed by western blotting with anti-NPM1 antibody (Figure 5C and D). Consistent with the data shown in Figure 1C, NPM1 was co-precipitated with full length p65. The N-terminal domain of p65 (p65-N1) that contains the DNA binding domain of p65, but not the dimer formation domain without or with the activation domain (p65-N2 or p65-N2C, respectively), co-precipitated with endogenous NPM1. The N-terminal domain with the dimer formation domain (p65-N) also efficiently co-precipitated NPM1, indicating that NPM1 interacts with the DNA binding domain of p65.

Because NPM1 interacts with the DNA binding domain, we next questioned whether the N-terminal domain is sufficient for NPM1 to enhance the DNA binding activity of p65. NPM1 increased the binding of p65-N to the κB DNA in a dose dependent manner (Figure 6A and B), suggesting that the C-terminal activation domain of p65 is dispensable for NPM1 to enhance the DNA binding activity of p65.

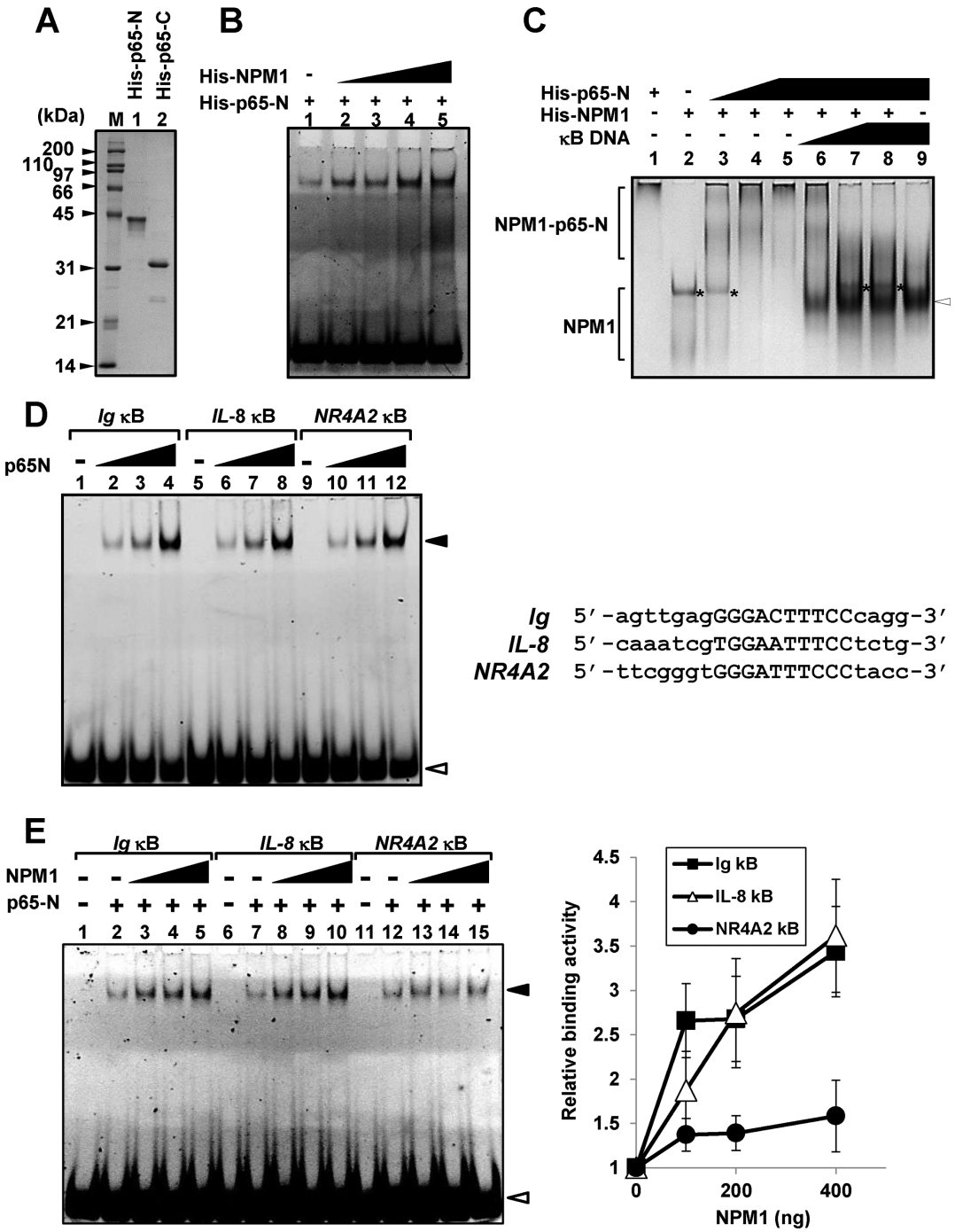

Figure 6. The chaperone-like function of NPM1 enhances the binding of p65 to specific sequences. (**A**) Purified proteins. His-p65-N and His-p65-C were separated by SDS-PAGE and visualized by CBB staining. (**B**) Effect of NPM1 on the DNA binding activity of p65-N. His-p65-N (40 ng, lane 1–5) were incubated with increasing amounts of His-NPM1 (0, 100, 200, 400 and 800 ng), and EMSA was performed. DNA was visualized by GelRed staining. (**C**) NPM1 and DNA complete for p65-N binding. His-NPM1 (60 pmole, lanes 2–8) was incubated with increasing amounts of His-p65-N (lanes 2–5, 0, 25, 50, 100 pmole, lanes 6–9, 100 pmole), then incubated without (lanes 1–5) or with increasing amounts of κB DNA (for lanes 6–8, 40, 80 and 160 pmole, respectively). Lanes 1 and 9 indicate His-p65-N alone (100 pmole) and the mixture of His-p65-N (100 pmole) and κB DNA (160 pmole), respectively. The complexes were separated by native PAGE and visualized by CBB staining. Positions of free NPM1 are shown at the left side of the panel and the accumulated free NPM1 is also indicated by asterisks at the right side of the lanes. (**D**) The binding of p65-N to different DNA probes. Three κB DNA fragments (2 pmole) derived from *Ig*, *IL-8* and *NR4A2* genes as shown at the right of the panel were incubated with increasing amounts of His-p65-N (0, 0.5, 1, 2 pmole, lanes 1–4, 5–8 and 9–12, respectively), separated by native PAGE and visualized by GelRed staining. The κB consensus sequences are indicated by capital letters. (**E**) NPM1 enhances the binding of p65-N to specific κB sites. The κB DNA fragments as in (D) were mixed with His-p65-N protein (0.5 pmole) pre-incubated with increasing amounts of His-NPM1 (0, 100, 200, 400, lanes 2–5, lanes 7–10, lanes 12–15), separated by native PAGE and visualized by GelRed staining. Lanes 1, 6 and 11 indicate the kB DNA fragments without p65-N or NPM1. The intensity of the bands for p65-N-DNA complex were quantitatively analyzed and shown at the right graph. The experiments were repeated five times and error bars indicate ±SD. Blank and filled arrowheads in D and E show free DNA probes and the p65-N–DNA complexes, respectively.

Given that NPM1 directly interacted with the DNA binding domain of p65 and that NPM1 was not incorporated into the NF-κB/DNA complex, it was speculated that NPM1 and DNA compete for the binding to NF-κB. This speculation was first examined by gel shift assay using purified p65-N and NPM1 (Figure 6C). NPM1 is an acidic protein and migrated to the cathode in native gel, whereas p65-N entered the gel inefficiently (lanes 1 and 2). The mobility of NPM1 was shifted upon addition of p65-N in a dose dependent manner (lanes 2–5). However, the addition of κB DNA increased free NPM1 and the DNA–p65-N complex appeared (lanes 6–8). Taken together, these results suggest that the chaperone-like function of NPM1 is required for the efficient DNA binding of NF-κB. To further confirm this conclusion, disruption of NPM1–p65-N complex by the κB DNA oligonucleotide was examined using purified proteins and oligonucleotide (Supplementary Figure S4). The p65-N protein bound to GST-NPM1 was eluted in the supernatant in an oligonucleotide concentration-dependent manner. Because the mutant κB DNA did not efficiently compete with NPM1 for the binding to p65-N, NPM1 transferred the p65-N protein preferentially to the κB DNA.

To clarify the mechanism by which NPM1 regulates a subset of NF-κB target genes, EMSA assays were performed using the κB site DNA fragments derived from *Ig*, *IL-8* and *NR4A2* genes (Figure 6D). The p65-N protein bound to all three κB site DNAs with similar efficiency. Interestingly, NPM1 significantly enhanced the binding of p65-N to *Ig* and *IL-8* κB sites, whereas the effect of NPM1 on the binding of p65-N to the *NR4A2* κB site was very low (Figure 6E). This result indicates that the κB sequence and/or the sequence around it determines the requirement of NPM1 for the efficient p65 binding to its target sites.

NPM1 decreases the intramolecular interaction of p65

It was previously reported that the intramolecular interaction between the N- and C-terminal domains of p65 blocks the binding of CBP/p300 to the p65 protein (41). This suggests that the formation of the transcription activation complex is controlled by the intramolecular interaction of p65. Considering that NPM1 interacts with the N-terminal domain of p65, we speculated that NPM1 might compete with the C-terminal domain of p65 for the binding to the N-terminal domain of p65, thus decreases the intramolecular interaction of p65 to enhance the assembly of the transcription activation complexes. To examine this, gel shift assay was performed using purified NPM1, p65-N and p65-C (Figure 7A). Free p65-C migrated to the cathode and the p65-C band was shifted upon addition of p65-N in its dose-dependent manner (lane 2–5), ensuring the interaction between p65-N and p65-C. Interestingly, the addition of NPM1 increased free p65-C (lanes 6–8) and the NPM1–p65-N complex appeared, indicating that NPM1 decreased the intramolecular interaction between p65-N and -C. From these results, it is suggested that the p65 subunit of NF-κB translocated to the nuclei upon various stimuli is bound by NPM1. NPM1 enhances the DNA binding of NF-κB via its chaperone-like function and simultaneously decreases the intramolecular interaction of p65 to enhance the assembly of the transcription activation complexes (Figure 7B).

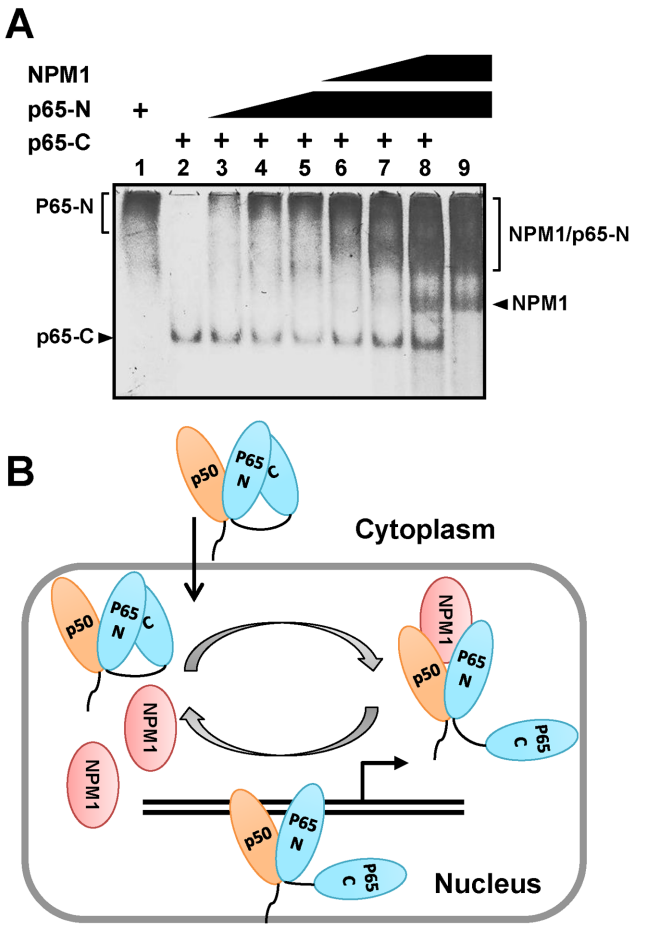

Figure 7. NPM1 decreases the intramolecular interaction of p65. (**A**) NPM1 decreases the interaction between p65-N and p65-C. His-p65-C (lanes 2–8, 12 pmole) was incubated with increasing amounts of His-p65-N (lanes 2–5, 0, 9, 27, 54 pmole and lanes 6–8, 54 pmole) and His-NPM1 (lanes 2–5, 0 pmol, lanes 6–8, 20, 40, 80 pmole), lane 1 indicates 54 pmole of His-p65-N alone, lane 9 indicates 80 pmole of His-NPM1 incubated with 54 pmole of His-p65-N. Proteins were separated by native PAGE and visualized by silver staining. (**B**) A working model of NF-κB-mediated transcription regulated by NPM1. Upon stimulation, NF-κB is translocated to the nucleus where it associates with NPM1. The association of NPM1 enhances the DNA binding activity of NF-κB and decreases the intramolecular interaction of p65. NPM1 releases NF-κB upon its binding to target DNA.

Functional intersection between NPM1 and NF-κB

Because NF-κB is a crucial regulator of tumor formation, progression and migration (42), and NPM1 is highly expressed in cancer cells (27), we next investigated the biological significance of the interaction between NF-κB and NPM1 in cancer. We first examined the expression of NPM1 and NF-κB in normal colon and adenomas obtained from multiple intestinal neoplasia (min) mice carrying a mutation in the *adenomatous polyposis coli* gene ($Apc^{min/+}$ mice) treated with dextran sodium sulfate, an inducer of colitis (Supplementary Figure S5A and Figure 8A). The normal colon epithelium (lower section of the pictures)

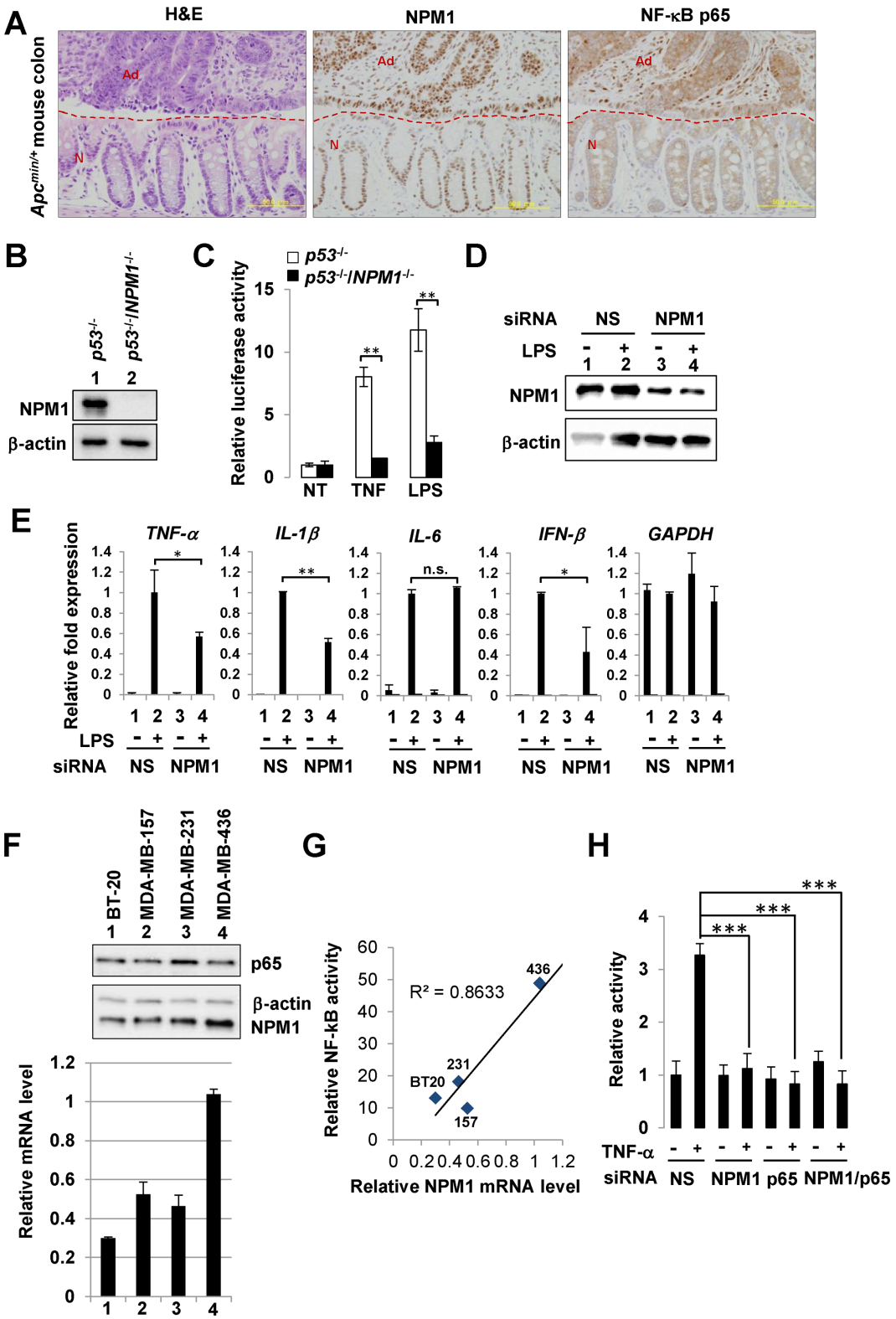

Figure 8. Functional intersection between NPM1 and NF-κB signaling. (**A**) Expression and localization of NPM1 and p65 in inflammatory colon in $Apc^{min/+}$ mice. Hematoxylin and eosin (HE) staining, and immunohistochemistry with anti-NPM1 and -p65 antibodies are shown as indicated. 'N' and 'Ad' represent normal and adenoma, respectively. Scale bars indicate 50 μm. (**B**) Western blotting of $p53^{-/-}$ and $p53^{-/-}NPM1^{-/-}$ MEFs with anti-NPM1 and anti-β actin. (**C**) The NF-κB-dependent reporter activity in MEFs. $p53^{-/-}$ and $p53^{-/-}NPM1^{-/-}$ MEFs were transfected with reporter plasmids for 16 h, stimulated without or with TNF-α (20 ng/ml) or LPS (1 μg/ml) for 3 h, and examined for luciferase activity. The relative NF-κB-driven luciferase activity (fold increase) is shown. Three independent experiments were performed and error bars are ± SD. (**D**) Western blotting of mouse peritoneal macrophages. Mouse peritoneal macrophages were transfected with NS or NPM1 siRNA for 72 h, followed by treatment with or without LPS (1 μg/ml)

showed uniform crypts, whereas the crypt structures were disorganized in the adenomas (upper section of the pictures). Hematoxylin and eosin (HE) staining clearly demonstrated that the cells in adenomas exhibited slightly larger nuclei, prominent nucleoli and intensely colored cytoplasm. We found that much stronger expression of both the p65 subunit of NF-κB and NPM1 was detected in adenomas than in normal colon. Both proteins were also detected at high levels in stromal cells. Importantly, p65 was mainly detected in the nucleus in stromal cells in adenomas, suggesting that NF-κB was activated in stromal cells.

Given that tumor cells are associated with a heterogeneous mixture of stromal cells that include fibroblasts and immune cells, it was possible that NPM1 and NF-κB cooperatively induce cancer progression by the functions of stromal cells. To examine this possibility, we tested the functional interaction between NPM1 and NF-κB in both MEFs and peritoneal macrophages. We used *p53*$^{-/-}$ and *p53*$^{-/-}$*NPM1*$^{-/-}$ MEFs to examine the effect of NPM1 depletion on the NF-κB-driven luciferase expression. *NPM1*$^{-/-}$ MEFs undergo cell cycle arrest due to p53 activation and can grow only when p53 is also depleted (43). Both TNF-α and LPS stimuli induced the NF-κB-driven luciferase activity in *p53*$^{-/-}$ control MEFs (Figure 8C). However, the reporter activities induced by both stimuli were significantly lower in *p53*$^{-/-}$*NPM1*$^{-/-}$ MEFs than those in *p53*$^{-/-}$ control MEFs (Figure 8C). Next, mouse peritoneal macrophages were treated with control or NPM1 siRNAs and the expression of NPM1 was examined by western blotting (Figure 8D). NPM1 expression was clearly decreased by NPM1 siRNA treatment, whereas that of actin was unchanged. The expressions of NF-κB target genes *TNF-α*, *IL-1β*, *IL-6* and *IFN-β*, but not *GAPDH*, were significantly induced by LPS (Figure 8E, lanes 1 and 2). The induced expressions of *TNF-α*, *IL-1β* and *IFN-β* were significantly decreased by NPM1 knockdown, whereas the expression of the *IL-6* gene was not significantly affected. Considered together, our results demonstrated that NPM1 and NF-κB cooperatively regulate the inflammatory responses both in fibroblasts and macrophages.

To address the significance of the interaction between NPM1 and p65 in cancer, we examined the effect of NPM1 on the expression of the NF-κB target genes in colon cancer cell line HCT-116 (Supplementary Figure S5B and C). NPM1 depletion decreased the expression of *IL-8*, *CCL2*, *CCL20* and *TNF-α*, suggesting that the functional interaction between NPM1 and NF-κB plays critical roles in colon cancer. Furthermore, we examined the expression level of NPM1 in various breast cancer cell lines using the GOBO database (44), because breast cancer cells having 'triple negative' phenotype, namely no expression of estrogen receptor, progesterone receptor and ERBB2, show constitutive activation of the NF-κB activity (45). Previous study showed that NPM1 is highly expressed in normal luminal epithelial cells and its expression is induced by hormones (46). However, among commonly used 51 breast cancer cell lines, the expression of NPM1 was highest in the basal B subtype cell lines that show 'triple negative' phenotype and exhibit a stem cell-like gene expression profile (47), and was the lowest in luminal subtype cell lines that show more differentiated and non-invasive phenotype (Supplementary Figure S6A and B) (47). To confirm the expression of NPM1 in basal A- or B-type breast cancer cell lines (BT20, MDA-MB-157, MDA-MB-231 and MDA-MB-436), RT-PCR and western blotting were performed (Figure 8F). The results indicated that the expression of NPM1 was the highest in MDA-MB436 cells among the four cell lines tested. The previously determined constitutive NF-κB activities of these cells (45) were plotted against NPM1 mRNA level (Figure 8G). The constitutive NF-κB activity was correlated with the expression level of NPM1, although the expression level of p65 was not very high in MDA-MB-436 cells (Figure 8H and G). These results support the idea that NPM1 is a positive regulator of the NF-κB complex.

Because NF-κB has been reported to regulate cancer cell migration and invasion (42), we examined the effect of NPM1 knockdown on TNF-α-induced cancer cell invasion by matrigel invasion assays using a breast cancer cell line, MDA-MB-231 (Supplementary Figure S7 and Figure 8H). We demonstrated that TNF-α treatment significantly enhanced the invasion of MDA-MB-231 cells. Upon knockdown of NF-κB p65, the TNF-α induced invasion of MDA-MB-231 cells was greatly reduced, indicating that the invasion enhanced by TNF-α was NF-κB-dependent. Knockdown of NPM1 or double knockdown of NPM1 and p65 both blocked the TNF-α-induced invasion, suggesting that NPM1 regulates cancer cell invasion through enhancing NF-κB signaling. The expression level of p65 and NPM1 by siRNA treatment was confirmed by western blotting (Supplementary Figure S7A). The expression of the chemokines *CCL2* and *CCL20*, which have been reported to regulate the migration of breast cancer cells (48,49), not *GAPDH,* were decreased by NPM1 knockdown (Supplementary Figure S7C). Considered together, we concluded that NPM1

←

for 2 h. The extracts were subjected to western blotting with anti-NPM1 and anti-β actin antibodies. (**E**) Expression of cytokine genes in macrophages. Total RNAs were extracted from cells as in (D) and the expressions of cytokines (*TNF-α, IL-1β*, *IL-6* and *IFN-β*) and *GAPDH* were analyzed by RT-qPCR. Three independent experiments were performed and error bars are ± SD. (**F**) Expression of NPM1 in breast cancer cell lines. Cell extracts (2 and 4 μg of proteins for top and middle panels, respectively) from BT-20, MDA-MB-157, MDA-MB-231 or MDA-MB-436 cells were separated by 10% SDS-PAGE and the expression of p65, β-actin and NPM1 was examined by western blotting. Total RNA was extracted and the expression of *NPM1* and *β-actin* was quantitatively analyzed by RT-qPCR. The amount of *NPM1* mRNA was normalized by that of *β-actin* and shown in bottom graph. (**G**) Relationship between the NF-κB activity and NPM1 expression level. The constitutive NF-κB activity obtained from published data (45) was plotted as a function of the NPM1 mRNA level shown in (F). (**H**) Invasion activity of MDA-MB-231 cells. MDA-MB-231 cells were transfected with NS, NPM1, p65, or NPM1 and p65 siRNAs for 48 h, seeded in transwells coated with Matrigel, and treated without or with TNF-α for 16 h. Representative images of the bottom surface are shown in Supplementary Figure S7B. Cell number detected at the bottom surface of control siRNA-treated and non-stimulated cells was set as 1.0, and relative cell numbers were quantitatively analyzed. Cell numbers were averages of four random microscopic fields from three independent experiments and error bars are ± SD. The results in C, E and H were statistically analyzed by student *t*-test and ***, ** and * indicates $P < 0.001$, 0.01 and 0.05, respectively.

and NF-κB cooperatively regulate the cancer progression induced by the NF-κB signaling.

DISCUSSION

In this study, we revealed the role of NPM1 in the NF-κB signaling pathway and examined the physiological significance of this role. The data presented here suggest a working model in which NPM1 interacts with NF-κB in the nucleus to stimulate the binding of NF-κB to target gene promoters. Interestingly, NPM1 itself disassociates from NF-κB once NF-κB binds to DNA (Figure 7B). NPM1 interacts with the N-terminal DNA binding domain of p65 and competes with DNA for the binding to p65, which results in the release of NPM1 after p65 binds to DNA. These results suggest that the chaperone-like function of NPM1 is required for the maximal transcription stimulatory activity of NF-κB. We also showed that NPM1 attenuates the intramolecular interaction between the N- and C-terminal domains of p65 (Figure 7A). The intramolecular interaction blocks the recruitment of transcriptional coactivators CBP/p300 (41). Thus, by decreasing the intramolecular interaction of p65, NPM1 may also enhance the interaction between p65 and CBP/p300 before p65 binds to DNA. We noted that although the expressions of some NF-κB target genes such as *PLAU* and *IL-8* were greatly decreased by NPM1 knockdown (Figure 2E), the recruitment of NF-κB p65 to the promoters was only decreased to about half (Figure 3C). Thus, it is possible that NPM1 regulates both the DNA binding and activator recruitment activities of the NF-κB proteins.

Our microarray and ChIP data indicated that NPM1 regulates a subset of NF-κB target genes induced by TNF-α (Figure 2). ChIP experiments revealed that NPM1 is required for the efficient recruitment of the NF-κB p65 to the inflammatory genes, whereas p65 was able to be recruited to the promoter regions of *NR4A2* and *DUSP5* independently of the NPM1 expression level (Figure 3C). This gene specific regulation by NPM1 could be explained by the result that NPM1 enhances the binding of p65 to specific κB sites (Figure 6E). Although the feature of sequence to which NPM1 enhances the binding of p65 is currently unclear, the κB sequence and/or the sequence around it affect the sequence specificity of p65 complexed with NPM1. These results also suggest that other NF-κB cofactor(s) might be involved in the regulation of these genes either by competing with NPM1 to bind to NF-κB or by compensating the function of NPM1 in NPM1 knockdown cells. For example, RPS3, cyclin-dependent kinase 6 and telomerase (13,15,16) have been found to be cofactors of NF-κB. It will be important to understand how these cofactors, including NPM1, cooperatively or independently regulate the NF-κB functions in inflammatory responses and cancer progression. In addition, five NF-κB proteins form various homo-dimers and hetero-dimers. Therefore, it is possible that NPM1 interacts with and stimulates the activity of specific NF-κB proteins. It was recently shown that *IL-6* expression in mouse macrophages is regulated by the I-κBξ–p50 complex that binds to a cofactor Akirin2 to recruit the SWI/SNF chromatin remodeling complex (50). Akirin2 does not interact with the p65 and NPM1 did not enhance the *IL-6* gene expression in macrophages (Figure 8E). Therefore, it is possible that NPM1 does not associate with or affect the activity of the I-κBξ–p50 complex in macrophages. Consistent with this, we demonstrated that NPM1 preferentially binds to the canonical NF-κB proteins p65 (Figure 1A and Supplementary Figure S1).

NF-κB mediated transcription does not simply depend on the amount of NF-κB. The post-translational modifications and co-factors, as well as the chromatin structure around their target genes contribute to determining the NF-κB activity. Precisely controlled NF-κB activity is required for normal cell growth and immune and inflammatory responses (51). NPM1 is broadly expressed in normal cells and is suggested to contribute to the maintenance of appropriate NF-κB activity as it was shown to regulate NF-κB-mediated transcription in fibroblasts and macrophages which are the components of tumor micro-environment (Figure 8C–E). In addition, NPM1 may potentially contribute to the oncogenic NF-κB functions in cancer cells as it regulates the NF-κB mediated transcription in cancer cells (Figures 2 and 8) and its expression level is correlated to NF-κB activity in colon adenoma and breast cancer cell lines (Figure 8). The results that NPM1 regulated NF-κB mediated inflammatory genes in both cancer cells and normal cells like macrophages suggest the oncogenic role of NPM1 in both tumor cells and the tumor microenvironment through the regulation of NF-κB. Considering that NPM1 also shows other oncogenic functions independent of NF-κB, such as regulating the activity and stability of p53 and ARF, cell growth, proliferation and anti-apoptosis, it is likely that the expression level of NPM1 is a suitable diagnostic marker to determine the aggressiveness of cancer cells and also a suitable target of cancer therapy.

SUPPLEMENTARY DATA

Supplementary Data are available at NAR Online.

ACKNOWLEDGEMENTS

We thank Dr Emanuela Colombo (European Institute of Oncology, Italy) for her kind gifts of $p53^{-/-}$ and $p53^{-/-}NPM1^{-/-}$ MEFs, Dr Kenkichi Masutomi (National Cancer Center Research Institute, Japan) for his gift of breast cancer cell lines, Dr Yukari Okita (University of Tsukuba, Japan) for her help to maintain the $Apc^{min/+}$ mice and immunohistochemistry analyses and Dr Youqiong Ye for her help to analyze the microarray data using the software *R*.

FUNDING

Grants-in-aid for Scientific Research from the Ministry of Education, Culture, Sports, Science, and Technology of Japan [26440021 to M. O., 25291001, 24115002 to K. N.]. Funding for open access charge: Ministry of Education, Culture, Sports, Science, and Technology of Japan [25291001, 24115002 to K. N.].

Conflict of interest statement. None declared.

REFERENCES

1. Foulds,L. (1954) The experimental study of tumor progression—a review. *Cancer Res.*, **14**, 327–339.

2. Hanahan,D. and Weinberg,R.A. (2011) Hallmarks of cancer: the next generation. *Cell*, **144**, 646–674.
3. Tredan,O., Galmarini,C.M., Patel,K. and Tannock,I.F. (2007) Drug resistance and the solid tumor microenvironment. *J. Natl. Cancer Inst.*, **99**, 1441–1454.
4. Wang,D.J., Ratnam,N.M., Byrd,J.C. and Guttridge,D.C. (2014) NF-kappaB functions in tumor initiation by suppressing the surveillance of both innate and adaptive immune cells. *Cell Rep.*, **9**, 90–103.
5. Pikarsky,E., Porat,R.M., Stein,I., Abramovitch,R., Amit,S., Kasem,S., Gutkovich-Pyest,E., Urieli-Shoval,S., Galun,E. and Ben-Neriah,Y. (2004) NF-kappaB functions as a tumour promoter in inflammation-associated cancer. *Nature*, **431**, 461–466.
6. Luo,J.L., Maeda,S., Hsu,L.C., Yagita,H. and Karin,M. (2004) Inhibition of NF-kappaB in cancer cells converts inflammation-induced tumor growth mediated by TNFalpha to TRAIL-mediated tumor regression. *Cancer Cell*, **6**, 297–305.
7. Greten,F.R., Eckmann,L., Greten,T.F., Park,J.M., Li,Z.W., Egan,L.J., Kagnoff,M.F. and Karin,M. (2004) IKKbeta links inflammation and tumorigenesis in a mouse model of colitis-associated cancer. *Cell*, **118**, 285–296.
8. Sen,R. and Baltimore,D. (1986) Multiple nuclear factors interact with the immunoglobulin enhancer sequences. *Cell*, **46**, 705–716.
9. Gilmore,T.D. (2006) Introduction to NF-kappaB: players, pathways, perspectives. *Oncogene*, **25**, 6680–6684.
10. Hayden,M.S. and Ghosh,S. (2012) NF-kappaB, the first quarter-century: remarkable progress and outstanding questions. *Genes Dev.*, **26**, 203–234.
11. Phelps,C.B., Sengchanthalangsy,L.L., Malek,S. and Ghosh,G. (2000) Mechanism of kappa B DNA binding by Rel/NF-kappa B dimers. *J. Biol. Chem.*, **275**, 24392–24399.
12. Zabel,U., Schreck,R. and Baeuerle,P.A. (1991) DNA binding of purified transcription factor NF-kappa B. Affinity, specificity, Zn2+ dependence, and differential half-site recognition. *J. Biol. Chem.*, **266**, 252–260.
13. Wan,F., Anderson,D.E., Barnitz,R.A., Snow,A., Bidere,N., Zheng,L., Hegde,V., Lam,L.T., Staudt,L.M., Levens,D. *et al.* (2007) Ribosomal protein S3: a KH domain subunit in NF-kappaB complexes that mediates selective gene regulation. *Cell*, **131**, 927–939.
14. Fu,K., Sun,X., Zheng,W., Wier,E.M., Hodgson,A., Tran,D.Q., Richard,S. and Wan,F. (2013) Sam68 modulates the promoter specificity of NF-kappaB and mediates expression of CD25 in activated T cells. *Nat. Commun.*, **4**, 1909.
15. Ghosh,A., Saginc,G., Leow,S.C., Khattar,E., Shin,E.M., Yan,T.D., Wong,M., Zhang,Z., Li,G., Sung,W.K. *et al.* (2012) Telomerase directly regulates NF-kappaB-dependent transcription. *Nat. Cell Biol.*, **14**, 1270–1281.
16. Handschick,K., Beuerlein,K., Jurida,L., Bartkuhn,M., Muller,H., Soelch,J., Weber,A., Dittrich-Breiholz,O., Schneider,H., Scharfe,M. *et al.* (2014) Cyclin-dependent kinase 6 is a chromatin-bound cofactor for NF-kappaB-dependent gene expression. *Mol. Cell*, **53**, 193–208.
17. Dhar,S.K., Lynn,B.C., Daosukho,C. and St Clair,D.K. (2004) Identification of nucleophosmin as an NF-kappaB co-activator for the induction of the human SOD2 gene. *J. Biol. Chem.*, **279**, 28209–28219.
18. Borer,R.A., Lehner,C.F., Eppenberger,H.M. and Nigg,E.A. (1989) Major nucleolar proteins shuttle between nucleus and cytoplasm. *Cell*, **56**, 379–390.
19. Okuwaki,M., Iwamatsu,A., Tsujimoto,M. and Nagata,K. (2001) Identification of nucleophosmin/B23, an acidic nucleolar protein, as a stimulatory factor for in vitro replication of adenovirus DNA complexed with viral basic core proteins. *J. Mol. Biol.*, **311**, 41–55.
20. Murano,K., Okuwaki,M., Hisaoka,M. and Nagata,K. (2008) Transcription regulation of the rRNA gene by a multifunctional nucleolar protein, B23/nucleophosmin, through its histone chaperone activity. *Mol. Cell. Biol.*, **28**, 3114–3126.
21. Savkur,R.S. and Olson,M.O. (1998) Preferential cleavage in pre-ribosomal RNA byprotein B23 endoribonuclease. *Nucleic Acids Res.*, **26**, 4508–4515.
22. Okuwaki,M., Sumi,A., Hisaoka,M., Saotome-Nakamura,A., Akashi,S., Nishimura,Y. and Nagata,K. (2012) Function of homo- and hetero-oligomers of human nucleoplasmin/nucleophosmin family proteins NPM1, NPM2 and NPM3 during sperm chromatin remodeling. *Nucleic Acids Res.*, **40**, 4861–4878.
23. Okuda,M., Horn,H.F., Tarapore,P., Tokuyama,Y., Smulian,A.G., Chan,P.K., Knudsen,E.S., Hofmann,I.A., Snyder,J.D., Bove,K.E. *et al.* (2000) Nucleophosmin/B23 is a target of CDK2/cyclin E in centrosome duplication. *Cell*, **103**, 127–140.
24. Koike,A., Nishikawa,H., Wu,W., Okada,Y., Venkitaraman,A.R. and Ohta,T. (2010) Recruitment of phosphorylated NPM1 to sites of DNA damage through RNF8-dependent ubiquitin conjugates. *Cancer Res.*, **70**, 6746–6756.
25. Okuwaki,M., Matsumoto,K., Tsujimoto,M. and Nagata,K. (2001) Function of nucleophosmin/B23, a nucleolar acidic protein, as a histone chaperone. *FEBS Lett.*, **506**, 272–276.
26. Falini,B., Mecucci,C., Tiacci,E., Alcalay,M., Rosati,R., Pasqualucci,L., La Starza,R., Diverio,D., Colombo,E., Santucci,A. *et al.* (2005) Cytoplasmic nucleophosmin in acute myelogenous leukemia with a normal karyotype. *N. Engl. J. Med.*, **352**, 254–266.
27. Grisendi,S., Mecucci,C., Falini,B. and Pandolfi,P.P. (2006) Nucleophosmin and cancer. *Nat. Rev. Cancer*, **6**, 493–505.
28. Zeller,K.I., Haggerty,T.J., Barrett,J.F., Guo,Q., Wonsey,D.R. and Dang,C.V. (2001) Characterization of nucleophosmin (B23) as a Myc target by scanning chromatin immunoprecipitation. *J. Biol. Chem.*, **276**, 48285–48291.
29. Tsui,K.H., Cheng,A.J., Chang,P., Pan,T.L. and Yung,B.Y. (2004) Association of nucleophosmin/B23 mRNA expression with clinical outcome in patients with bladder carcinoma. *Urology*, **64**, 839–844.
30. Hisaoka,M., Nagata,K. and Okuwaki,M. (2014) Intrinsically disordered regions of nucleophosmin/B23 regulate its RNA binding activity through their inter- and intra-molecular association. *Nucleic Acids Res.*, **42**, 1180–1195.
31. Steffensen,I.L., Paulsen,J.E., Eide,T.J. and Alexander,J. (1997) 2-Amino-1-methyl-6-phenylimidazo[4,5-b]pyridine increases the numbers of tumors, cystic crypts and aberrant crypt foci in multiple intestinal neoplasia mice. *Carcinogenesis*, **18**, 1049–1054.
32. Hisaoka,M., Ueshima,S., Murano,K., Nagata,K. and Okuwaki,M. (2010) Regulation of nucleolar chromatin by B23/nucleophosmin jointly depends upon its RNA binding activity and transcription factor UBF. *Mol. Cell. Biol.*, **30**, 4952–4964.
33. Hisaoka,M., Nagata,K. and Okuwaki,M. (2014) Intrinsically disordered regions of nucleophosmin/B23 regulate its RNA binding activity through their inter- and intra-molecular association. *Nucleic Acids Res.*, **42**, 1180–1195.
34. Gentleman,R.C., Carey,V.J., Bates,D.M., Bolstad,B., Dettling,M., Dudoit,S., Ellis,B., Gautier,L., Ge,Y., Gentry,J. *et al.* (2004) Bioconductor: open software development for computational biology and bioinformatics. *Genome Biol.*, **5**, R80.
35. Gautier,L., Cope,L., Bolstad,B.M. and Irizarry,R.A. (2004) affy—analysis of Affymetrix GeneChip data at the probe level. *Bioinformatics*, **20**, 307–315.
36. Irizarry,R.A., Bolstad,B.M., Collin,F., Cope,L.M., Hobbs,B. and Speed,T.P. (2003) Summaries of Affymetrix GeneChip probe level data. *Nucleic Acids Res.*, **31**, e15.
37. Irizarry,R.A., Hobbs,B., Collin,F., Beazer-Barclay,Y.D., Antonellis,K.J., Scherf,U. and Speed,T.P. (2003) Exploration, normalization, and summaries of high density oligonucleotide array probe level data. *Biostatistics*, **4**, 249–264.
38. Huang,D.W., Sherman,B.T., Tan,Q., Collins,J.R., Alvord,W.G., Roayaei,J., Stephens,R., Baseler,M.W., Lane,H.C. and Lempicki,R.A. (2007) The DAVID Gene Functional Classification Tool: a novel biological module-centric algorithm to functionally analyze large gene lists. *Genome Biol.*, **8**, R183.
39. Huang,D.W., Sherman,B.T., Tan,Q., Kir,J., Liu,D., Bryant,D., Guo,Y., Stephens,R., Baseler,M.W., Lane,H.C. *et al.* (2007) DAVID Bioinformatics Resources: expanded annotation database and novel algorithms to better extract biology from large gene lists. *Nucleic Acids Res.*, **35**, W169–W175.
40. Sun,S.C., Ganchi,P.A., Ballard,D.W. and Greene,W.C. (1993) NF-kappa B controls expression of inhibitor I kappa B alpha: evidence for an inducible autoregulatory pathway. *Science*, **259**, 1912–1915.
41. Zhong,H., Voll,R.E. and Ghosh,S. (1998) Phosphorylation of NF-kappa B p65 by PKA stimulates transcriptional activity by promoting a novel bivalent interaction with the coactivator CBP/p300. *Mol. Cell*, **1**, 661–671.
42. Karin,M. (2006) Nuclear factor-kappaB in cancer development and progression. *Nature*, **441**, 431–436.

43. Colombo,E., Bonetti,P., Lazzerini Denchi,E., Martinelli,P., Zamponi,R., Marine,J.C., Helin,K., Falini,B. and Pelicci,P.G. (2005) Nucleophosmin is required for DNA integrity and p19Arf protein stability. *Mol. Cell. Biol.*, **25**, 8874–8886.
44. Ringner,M., Fredlund,E., Hakkinen,J., Borg,A. and Staaf,J. (2011) GOBO: gene expression-based outcome for breast cancer online. *PLoS One*, **6**, e17911.
45. Yamaguchi,N., Ito,T., Azuma,S., Ito,E., Honma,R., Yanagisawa,Y., Nishikawa,A., Kawamura,M., Imai,J., Watanabe,S. *et al.* (2009) Constitutive activation of nuclear factor-kappaB is preferentially involved in the proliferation of basal-like subtype breast cancer cell lines. *Cancer Sci.*, **100**, 1668–1674.
46. Karhemo,P.R., Rivinoja,A., Lundin,J., Hyvonen,M., Chernenko,A., Lammi,J., Sihto,H., Lundin,M., Heikkila,P., Joensuu,H. *et al.* (2011) An extensive tumor array analysis supports tumor suppressive role for nucleophosmin in breast cancer. *Am. J. Pathol.*, **179**, 1004–1014.
47. Neve,R.M., Chin,K., Fridlyand,J., Yeh,J., Baehner,F.L., Fevr,T., Clark,L., Bayani,N., Coppe,J.P., Tong,F. *et al.* (2006) A collection of breast cancer cell lines for the study of functionally distinct cancer subtypes. *Cancer Cell*, **10**, 515–527.
48. Fang,W.B., Jokar,I., Zou,A., Lambert,D., Dendukuri,P. and Cheng,N. (2012) CCL2/CCR2 chemokine signaling coordinates survival and motility of breast cancer cells through Smad3 protein- and p42/44 mitogen-activated protein kinase (MAPK)-dependent mechanisms. *J. Biol. Chem.*, **287**, 36593–36608.
49. Marsigliante,S., Vetrugno,C. and Muscella,A. (2013) CCL20 induces migration and proliferation on breast epithelial cells. *J. Cell Physiol.*, **228**, 1873–1883.
50. Tartey,S., Matsushita,K., Vandenbon,A., Ori,D., Imamura,T., Mino,T., Standley,D.M., Hoffmann,J.A., Reichhart,J.M., Akira,S. *et al.* (2014) Akirin2 is critical for inducing inflammatory genes by bridging I kappa B-zeta and the SWI/SNF complex. *EMBO J.*, **33**, 2332–2348.
51. Pasparakis,M., Luedde,T. and Schmidt-Supprian,M. (2006) Dissection of the NF-kappaB signalling cascade in transgenic and knockout mice. *Cell Death Differ.*, **13**, 861–872.